STATIC AND FATIGUE ANALYSIS OF AN UPPER WING SKIN WITH EXFOLIATION CORROSION

Guillaume Renaud*, Min Liao*, Andreas Uebersax, Cyril Huber****
***National Research Council Canada, ****RUAG Aerospace**

Keywords: *exfoliation corrosion, life prediction, Al 7075, FEA, upper wing skin*

Abstract

This paper presents the modeling aspects of a collaborative research program on the effects of exfoliation corrosion and grindout repairs on the structural integrity of an upper wing skin. Finite element and fatigue models were developed to simulate exfoliation corrosion damages and grindout repairs located at fastener holes. Modeling and simulation of 19 test coupons of various exfoliation or grindout levels were carried out. Comparison with experimental data showed the usefulness of the proposed models to assess performance reduction.

1 Introduction

Exfoliation corrosion is a severe form of inter-granular corrosion. Like corrosion pitting and stress corrosion cracking, it is commonly found in wing skins made of aluminum alloys [1]. In the presence of exfoliation corrosion, operators face questions about the possible effects that exfoliation and the subsequent repairs have on the structural integrity, acceptable damage severity, and risk. For example, studies have shown that for certain levels of exfoliation the minimum required grindout repair may reduce the static strength and fatigue life more than the corrosion itself [2].

In the past years, extensive research on aircraft corrosion, including exfoliation, has been carried out at the National Research Council of Canada (NRC) [3]. Among several other techniques, automatic parametric FE modeling and crack growth simulation techniques were used to simulate testing of components comprising of exfoliation corrosion of different shapes and depths [4][5].

A collaborative project between NRC and RUAG Aerospace of Switzerland was undertaken to study the effects of exfoliation at fastener holes on the residual life of the upper wing skin of a fighter aircraft. This project includes both experimental and analytical aspects. For the analytical work, presented in this paper, a medium-complex geometric model was developed to represent the corrosion damage configuration. The damage was seen as an off-center rotatable truncated ellipsoid that enclosed a fastener hole. The corrosion damage was modeled as a "soft inclusion" with adjustable stiffness that can retain some load bearing capability. If the inclusion was removed and the fastener head was moved down, the model was representative of a grindout repair. Stress distributions obtained from static analysis were used as input data for fatigue analysis in order to quantify the effects that exfoliation corrosion or grindout repair had on residual strength and remaining fatigue life of the wing.

Analytical results of 19 test coupons with various exfoliation or repair characteristics are presented and compared with experimental data, and a quick performance reduction assessment method is suggested.

2 Static Analysis Model

A parameterized geometric and Finite Element (FE) model was developed for the static analysis of tapered wing skin test coupons comprising of exfoliation corrosion or grindout at the fastener hole. This model was implemented in MSC/PATRAN Command Language (PCL) to

automatically build MSC/MARC input files with the particular test article specifications.

2.1 Soft Inclusion Concept

The exfoliation damage was modeled as an inclusion of reduced stiffness. One of the underlying assumptions of this concept is that the exfoliation zone may retain some load carrying capability, depending on the corrosion level and the presence of deep inter-granular corrosion. For the model used in this work, the exfoliation zone was assumed isotropic and uniform, with a stiffness defined as a fraction reduction of the pristine material stiffness.

2.2 General Geometric Model

A medium-complex geometric model was developed to represent the corrosion damage or grindout. The corrosion or grindout was seen as a rotatable truncated ellipsoid that enclosed a fastener hole. The user-defined variables of the model included:

- coupon geometry variables (tapered thickness, width(s), length(s), radius);
- damage / grind-out geometry variables (ellipsoid short and long axes, maximum depth, position, rotation angle);
- rivet hole geometry variables (diameter, countersink depth and angle).

The geometric model of a typical specimen with corrosion is shown in Fig. 1 and the cross-sectional view of a mesh in the hole area is shown in Fig. 2.

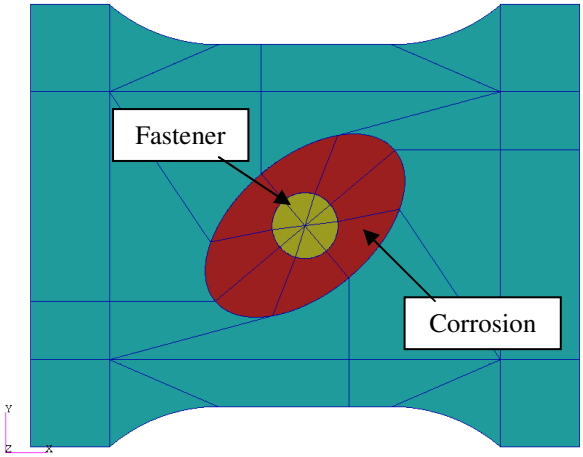

Fig. 1. Typical geometric model with corrosion.

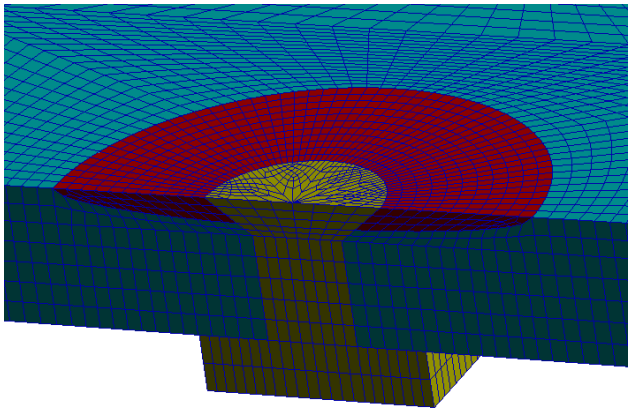

Fig. 2. Meshed hole area with corrosion (cross-section).

2.2.1 Corrosion Geometric Model

To cover the cases where the corrosion damage did not fully enclose the rivet hole, it was assumed that the 8 "quadrants" of the corrosion ellipsoid could be individually selected as corroded or pristine. Modeling examples of this type of corrosion damage are shown in Fig. 3.

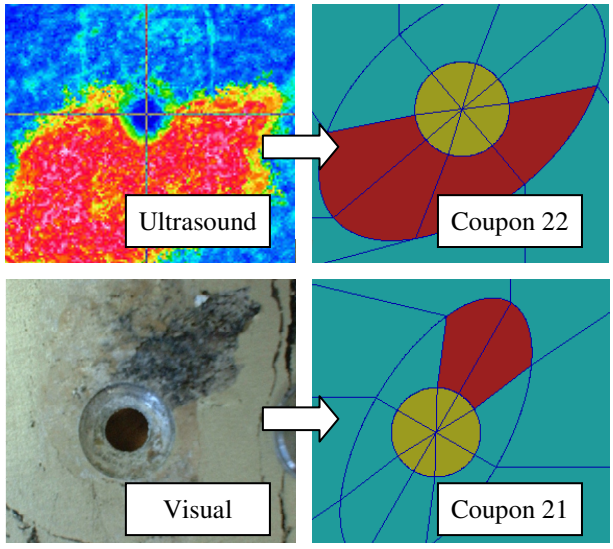

Fig. 3. Corrosion damage modeling examples.

The corrosion models presented in this paper are based on visual observation of the corroded area, and ultrasound measurements of the maximum thickness loss.

2.2.2 Grindout Geometric Model

The grindout repairs were modeled based on maximum depth and grindout diameter. In the specimens considered in this study, the grindout area was intentionally centered on the hole and made circular. As opposed to the corrosion model, the truncated ellipsoid was completely

removed from the model. Also, to consider the repositioning of the rivet head at the bottom of the groundout area, the countersunk hole was relocated at the bottom of the ellipsoid. A cross-sectional view of a mesh in the hole area of a grindout model is shown in Fig. 4.

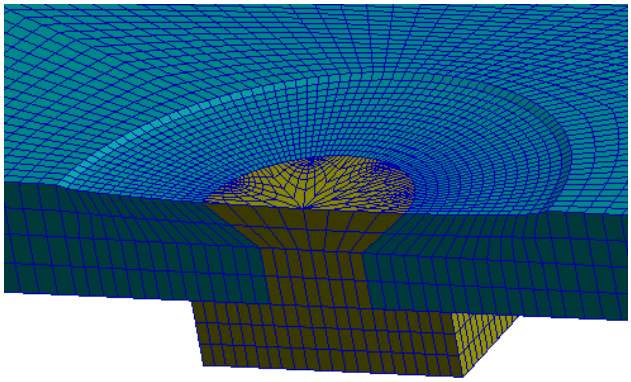

Fig. 4. Mesh hole area with grindout (cross-section).

2.2.3 Pristine Coupons Geometric Model

The pristine coupons were modeled exactly as the corroded ones, with arbitrary damage zone variables and all 8 ellipsoid "quadrants" assumed pristine.

2.3 Finite Element Model

The dogbone coupons were modeled using three-dimensional finite elements, assuming geometric nonlinearities (large deformations) and contact nonlinearities at the hole-rivet interface.

Material properties of 7075-T651 aluminum and steel were used for the pristine and fastener materials, respectively. As a first assumption, the corroded material was assumed to be isotropic, with a uniform 70% stiffness reduction with respect to the pristine material. This reduction value was determined in a previous project, using the same material, with a detailed exfoliation damage representation based on high resolution ultrasound thickness measurement scans [6].

The loads and boundary conditions were setup to match the test grip restrains and force.

Meshing parameters were used to ensure consistent element size around the hole for all the models. Examples of the mesh are shown in Fig. 2 and Fig. 4.

3 Fatigue Analysis Model

The crack growth model was developed in AFGROW for fatigue analysis of the coupons. The presence of corrosion damage or grindout repair was introduced by the use of spectrum modifications and stress correction factors calculated from the static analysis results. A base model, representative of the average test article, was developed both in AFGROW and MSC/MARC. The selected configuration consisted of a representative uniform thickness coupon with a filled unloaded center hole and the 7075-T6 Al NASGRO equation available in AFGROW was used as the material model for crack growth.

3.1 Beta Correction

The correction factors were inputted in the fatigue model using the normalized stress method in AFGROW. For each static model, maximum static tension and compression cases, based on the spectrum and load levels assigned to the specimen, were solved to determine the maximum principal stress curves emanating from the hole, in the plane of the specimen and along its thickness, and its associated minimum principal curves. For most cases, the maximum stress was located at the bottom of the countersink angle, at one or both of the natural maximum stress concentration points. An example of maximum principal stress distribution in the vicinity of a groundout hole is shown in Fig. 5.

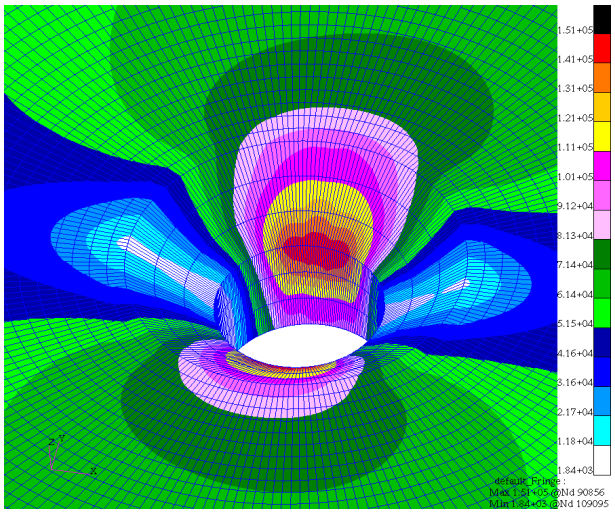

Fig. 5. Max. principal stress at a groundout hole.

The principal stress curves in both directions were compared with that of the base configuration in order to calculate the normalized stress Beta correction factor curves to be used in AFGROW. In so doing, it was assumed that the stress distributions considered in the AFGROW filled hole model were close to that obtained from the MSC/MARC contact analysis solution. The stress correction factor curve in the thickness direction introduced the bending caused by the neutral axis offset, due to the corrosion, grindout, and countersink hole.

In the present case, because of the nonlinear nature of the problem due to the fastener contact, normalized tension and compression stress curves were different. It was therefore impossible, by using a single stress correction curve, to set in AFGROW both the tension and compression stress curves obtained from the FE models. The chosen approach was to match the entire tension stress distributions, using the tension stress correction curve, and to match the maximum compression stress point, resulting in higher compressive stress over most of the coupon. To do so, the Stress Multiplication Factor (SMF) and the spectrum positive limit were adjusted. An illustration of typical stress curves is presented in Fig. 6.

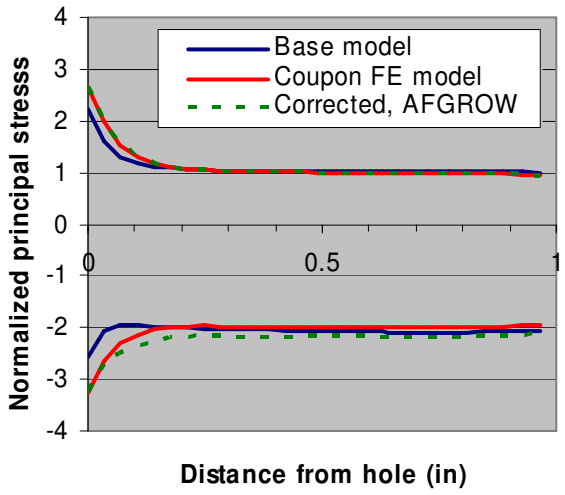

Fig. 6. Typical base, coupon, and corrected stress curves.

4 Test Program

Twenty-five wing skin test coupons with various characteristics were tested at RUAG Aerospace and NRC. This set of coupons included specimens that were pristine, naturally corroded, artificially corroded, and repaired by grindout. All coupons were taken from a retired fighter wing, which had 2101 flight hours in service. A list of the specimens is presented in Table 1.

Table 1. Test specimen list.

Specimen Number	Type	Maximum Thickness Loss
16, 18, 24, 25, 27	Pristine	0%
01, 04, 05, 10, 19, 23	Natural corrosion	N/A
06	0.5 mm grindout	8%
08	0.5 mm grindout	10%
11	0.5 mm grindout	11%
02	1.3 mm grindout	18%
12	1.3 mm grindout	39%
13	1.3 mm grindout	21%
07	2.0 mm grindout	26%
09	2.0 mm grindout	24%
14	2.0 mm grindout	29%
15	Artificial corrosion	7%
20	Artificial corrosion	26%
21	Artificial corrosion	5%
22	Artificial corrosion	34%
26	Artificial corrosion	26%

It can be seen that the maximum thickness loss percentage, based on the average thickness of the tapered specimen, ranged from 0% (pristine) to 39% (grindout). Moreover, the shape and size of the damage or repair were different for each specimen.

The natural corrosion specimens all had low corrosion levels, comparable to the pristine specimens. The artificial corrosion specimens were created using the ANCIT corrosion protocol to generate higher corrosion levels.

Load levels were determined for each specimen to ensure consistent stress in the hole area. The specimens were tested in fatigue under a compression-dominant upper wing skin fighter loading spectrum. Most of them reached 6 lives (4000 simulated flight hours / 232060 cycles per life) before failure. The available crack growth data and total life of the specimens that failed from the center hole were used for comparisons with analysis results.

A summary of the fatigue test results are presented in Fig. 7.

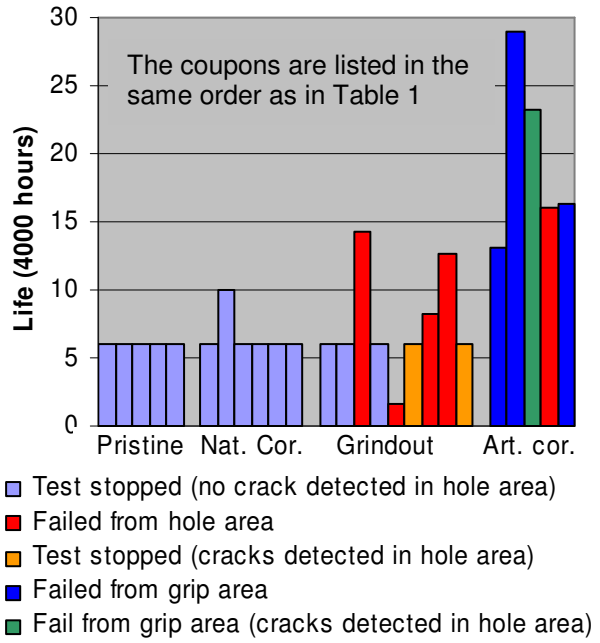

Fig. 7. Stress concentration vs. maximum thickness loss.

It can be seen that out of all the tested coupons, only the groundout specimens exhibited failure or cracking in the center hole region before the 6 lives test limit was reached. The only corroded specimen that failed was the one with the highest thickness loss (34%), at 16.03 lives.

Preliminary fractography showed that, for the grindout specimens, most of the cracks started from the top area of the countersunk hole. As indicated in Fig. 8, multiple crack nucleation sites were also identified on the grindout coupons. However, some nucleation features on the fracture surfaces were destroyed due to the compression loading.

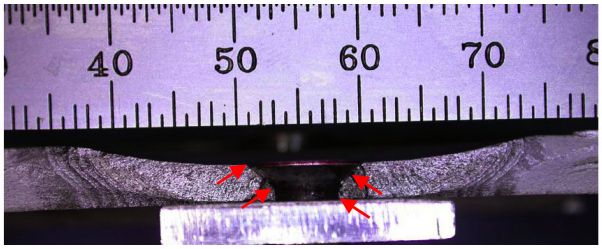

Fig. 8. Fracture surface with observed nucleation sites.

5 Analysis Results

All specimens but the natural corroded ones were modeled and analyzed in static tension, static compression, and fatigue, resulting in 19 distinct FE models, AFGROW models, stress modification curves, and modified load spectra.

5.1 Static Stress Analysis

Maximum tension and compression tests were simulated for all specimens. A summary of the maximum and minimum principal stress values, normalized over the nominal gross section applied stress, defined as stress concentration factors, is presented in Fig. 9.

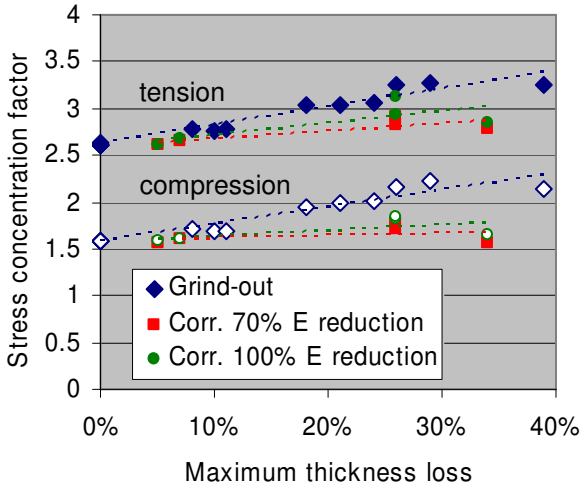

Fig. 9. Stress concentration vs. maximum thickness loss.

It is seen in Fig. 9. that the stress concentration factors are well correlated with the grindout thickness loss. Also, for equivalent thickness loss, the corroded specimen exhibit lower stress concentration factors than the grindout ones. This is mainly due to the assumed residual stiffness in the exfoliation area, and to the possibility of having a deep but small corrosion damage area, located away from the maximum stress concentration point. Consequently, the stress to thickness loss relation is weaker for the corroded specimens, which would need additional metrics, such as corrosion volume and location with respect to the load direction, to be adequately quantified. It is also seen that changing the stiffness of the soft inclusion does not affect the stress concentration uniformly for all specimens, principally because of the different shapes and sizes of the various corrosion damages.

5.2 Fatigue Analysis

The chosen calibration method for the fatigue analysis model was to adjust the initial crack size in order to match the total fatigue lives and crack growth data observed in the tests. No retardation was assumed.

From the fatigue tests, only specimens 7, 9, and 11 provided usable crack growth information. The crack grew from both sides of the hole for the 3 specimens. Therefore, the initial crack model in AFGROW was selected as a quarter-circular double corner crack at a hole. This crack model is represented in Fig. 10 for a grindout geometry.

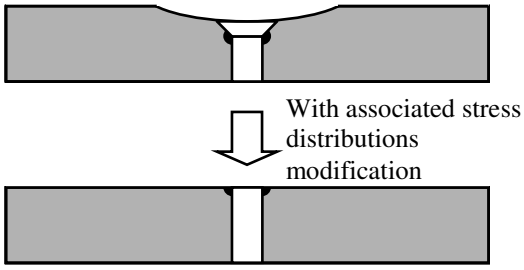

Fig. 10. Crack model for a grindout geometry.

An initial crack size of 0.004" was found to provide a reasonable match with the total fatigue lives and available crack growth data. A comparison between the analytical and experimental crack growth, from both sides of the hole, is presented in Fig. 11.

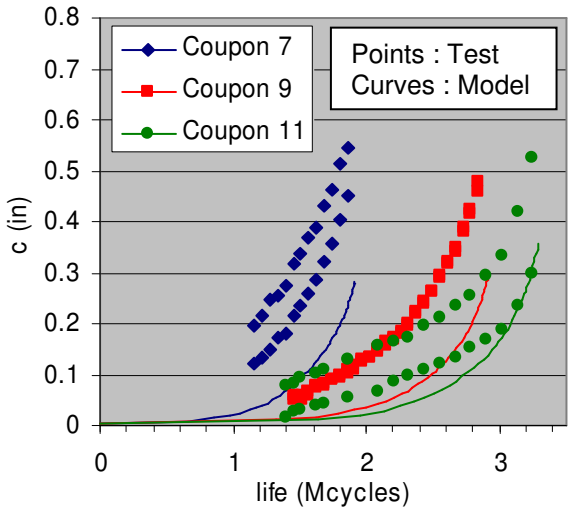

Fig. 11. Experimental and analytical crack growth.

The calibrated initial crack size of 0.004" was used to compare the calculated analytical lives with the experimental results. The comparison with the test life of coupons that failed from the center hole is presented in Fig. 12.

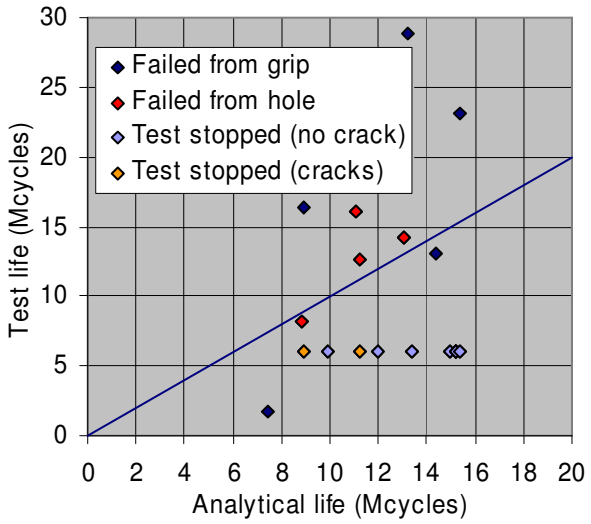

Fig. 12. Analytical and test lives comparison.

Since testing of most coupons was stopped at 6 lives, limited data is available to evaluate the quality of the calibrated model. However, it can be seen that the model seems to be on the conservative side, only one test coupon having failed, unexpectedly and without crack growth recorded, significantly before the model prediction. A summary of all analytical lives, plotted against maximum thickness loss, is presented in Fig. 13.

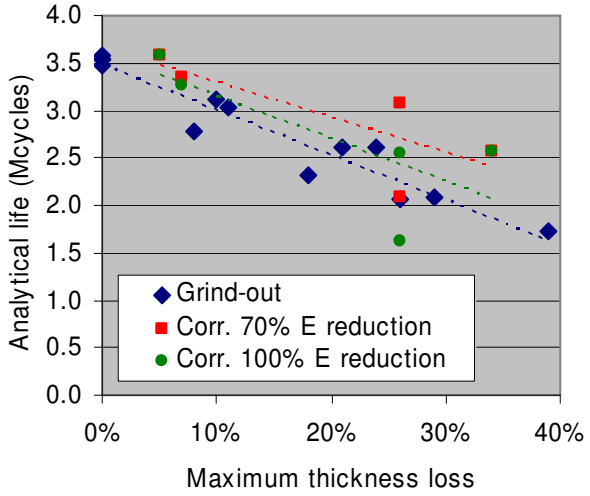

Fig. 13. Analytical life vs. maximum thickness loss.

It is seen that the analytical life of the grindout specimens is well correlated with the maximum thickness loss. However, this sole parameter does not provide such a good correlation with the analytical life of the corroded specimens. For example, it is seen that the analytical life of one of the corroded coupons was lower than a groundout coupon of equivalent thickness loss. This is mainly due to the extensive corroded area and bending field associated with that particular corrosion damage.

5 Engineering Considerations

Curves like those presented in Fig. 9 and Fig. 13 could be used in an engineering context for a quick assessment of the effects of exfoliation corrosion and guidance on possible grindout actions. Using such curves, calibrated for various initial crack sizes, an engineer could carry out a quick damage tolerance analysis. For example, the performance reductions, with respect to the pristine state, resulting from the 0.05" initial crack standard assumption and a thickness loss of 10%, are listed in Table 2.

Table 2. Effects of a 10% thick. loss (0.05"initial crack).

Assumption	Stress concentration factor increase	Life reduction
Corrosion 70% red.	2.5%	3.1%
Corrosion 90% red.	3.1%	7.2%
Grindout	7.6%	13.5%

The results presented in Table 2 were based on the assumption that the grindout geometry, that of coupon 8 in this example, is identical to the corrosion geometry. This is a conservative assumption since the grindout of corrosion damage always removes more material. Furthermore, any grindout action, especially outside a controlled laboratory environment, is likely to create machining marks, which are potential nucleation sites. The table suggests that, for the structural location studied and loading spectrum applied, it may be beneficial/preferable to leave a certain level of corrosion instead of grinding it out. It should be noted that different stress increases and life reductions would be obtained if other initial crack lengths were assumed.

6 Conclusion

A combination of static and fatigue analysis models were developed to evaluate the impact of exfoliation and grindout repair on residual strength and remaining fatigue life of dogbone test coupons. A total of 19 specimens were modeled and analyzed. A medium-complex geometric model, associated with the soft inclusion concept, was used for the corroded coupons modeling. Results showed that the models provided good estimation of the performance reduction due to exfoliation or grindout.

For the considered centered circular grindout repairs, the stress concentration and analytical life could be correlated directly to the maximum thickness loss. Such a direct relationship was not observed as clearly with the corroded specimens. A combined severity parameter, including the effects of maximum thickness loss, total corrosion volume, and damage location, is needed to give a better estimation of the performance of the corroded specimens.

Calibration of the models, both for the corrosion material properties and crack growth model (initial crack size, retardation), is of primary importance for quality analysis results. Sensitivity analysis on each input should be envisaged.

Once calibrated, the developed models could provide an engineering tool for quick assessment on the effects of corrosion damage on wing skins and guidance on possible grindout repair actions.

7 Acknowledgements

This project was supported by a RUAG-NRC collaborative project. On the NRC side, thanks to T. Benak and A. Marincak for fatigue testing, M. Brother for NDI, D. Backman for image correlation measurement and R. Desnoyers for fractography. Special thanks to N. Bellinger for

technical guidance, insightful discussion and critical review of this paper.

RUAG Aerospace would like to thank the following people for their support: M. Wyss for fatigue testing, J. Lussi and S. Zehnder for NDI. RUAG Aerospace would also like to give special thanks to armasuisse who provided funding for this project.

References

[1] Wallace W and Hoeppner DW. Aircraft corrosion: Causes and case histories. *AGARD Corrosion Handbook*, Vol. 1, AGARD-AG-278, p 93, 1985.

[2] Worsfold M. The effect of corrosion on the structural integrity of commercial aircraft structure. *The NATO Applied Vehicle Technology Panel*, Corfu, Greece, 2001.

[3] Komorowski JP, Bellinger NC, Gould RW, Forsyth D and Eastaugh G. Research in corrosion of ageing transport aircraft structures at SMPL. *Canadian Aeronautics and Space Journal*, Vol. 47, 2001, pp 1-11.

[4] Liao M, Renaud G, Backman D, Forsyth DS and Bellinger NC. Modeling of prior exfoliation corrosion in aircraft wing skins. *2nd International Conference on Environment-Induced Cracking of Metals*, Banff, Alberta, 2004.

[5] Liao M, Renaud G, Bellinger NC, Backman D and Forsyth DS. Effects of exfoliation corrosion on static and fatigue behavior of aircraft materials and structures - Testing and modeling studies. *8th Joint NASA/FAA/DoD Conference on Aging Aircraft*, Palm Springs, California, 2005.

[6] Renaud G and Liao M. Finite element modeling of exfoliation corrosion. *NRC LTR-SMPL-2007-0120*, 2007.

Copyright Statement